

Selective Coke Combustion by Oxygen Pulsing During Mo/ZSM-5-Catalyzed Methane Dehydroaromatization

Kosinov, Nikolay; Coumans, Ferdy J A G; Uslamin, Evgeny; Kapteijn, Freek; Hensen, Emiel J M

DOI

[10.1002/anie.201609442](https://doi.org/10.1002/anie.201609442)

Publication date

2016

Document Version

Final published version

Published in

Angewandte Chemie (International Edition)

Citation (APA)

Kosinov, N., Coumans, F. J. A. G., Uslamin, E., Kapteijn, F., & Hensen, E. J. M. (2016). Selective Coke Combustion by Oxygen Pulsing During Mo/ZSM-5-Catalyzed Methane Dehydroaromatization. *Angewandte Chemie (International Edition)*, 55(48), 15086-15090. <https://doi.org/10.1002/anie.201609442>

Important note

To cite this publication, please use the final published version (if applicable). Please check the document version above.

Copyright

Other than for strictly personal use, it is not permitted to download, forward or distribute the text or part of it, without the consent of the author(s) and/or copyright holder(s), unless the work is under an open content license such as Creative Commons.

Takedown policy

Please contact us and provide details if you believe this document breaches copyrights. We will remove access to the work immediately and investigate your claim.

Methane Dehydroaromatization

International Edition: DOI: 10.1002/anie.201609442
German Edition: DOI: 10.1002/ange.201609442

Selective Coke Combustion by Oxygen Pulsing During Mo/ZSM-5-Catalyzed Methane Dehydroaromatization

Nikolay Kosinov,* Ferdy J. A. G. Coumans, Evgeny Uslamin, Freek Kapteijn, and Emiel J. M. Hensen*

Abstract: Non-oxidative methane dehydroaromatization is a promising reaction to directly convert natural gas into aromatic hydrocarbons and hydrogen. Commercialization of this technology is hampered by rapid catalyst deactivation because of coking. A novel approach is presented involving selective oxidation of coke during methane dehydroaromatization at 700 °C. Periodic pulsing of oxygen into the methane feed results in substantially higher cumulative product yield with synthesis gas; a H₂/CO ratio close to two is the main side-product of coke combustion. Using ¹³C isotope labeling of methane it is demonstrated that oxygen predominantly reacts with molybdenum carbide species. The resulting molybdenum oxides catalyze coke oxidation. Less than one-fifth of the available oxygen reacts with gaseous methane. Combined with periodic regeneration at 550 °C, this strategy is a significant step forward, towards a process for converting methane into liquid hydrocarbons.

Natural gas is the cleanest of fossil energy resources in terms of CO₂ emissions per unit energy generated. Yet, it is of little value unless it can be brought from the well to the customer, who is usually very far away from the source. The low volumetric energy density of natural gas makes it difficult to transport. As a result of the high cost of transport (for example, pipelines and liquefaction), a significant fraction of natural gas reserves is considered “stranded”. Gas associated with oil exploration is another source of natural gas available for monetization, which is currently mostly flared.^[1] Aside from oxidative methane coupling, dehydroaromatization into benzene has received widespread attention as a promising technology for the upgrading of methane—the main

component of natural gas—into transportable liquids.^[2] There are two major drawbacks to this process, which were first described by Bragin et al. in the late 1980s.^[3] First, non-oxidative conversion of methane is met by unfavorable thermodynamics. Reasonable methane conversion is achieved only above 650 °C. At a typical temperature of 700 °C, the equilibrium conversion for non-oxidative methane conversion to benzene is about 12%, while graphitic/polyaromatic carbon (coke) is the thermodynamically favored product in a wide temperature range.^[4] Placing Mo-carbides, the most suitable catalyst for activating methane, inside the shape-selective pores of 10-membered ring zeolites such as MFI (Mo/ZSM-5) and MWW (Mo/MCM-22) is a prerequisite for obtaining reasonable benzene selectivity (50–80%).^[2a] The resulting Mo/zeolite composite is assumed to operate in a bifunctional manner; molybdenum species activate methane and couple the resulting CH_x fragments to form ethylene, which is subsequently oligomerized and aromatized to benzene and other aromatics on the zeolite acid sites.^[2b] Furthermore, the low thermal stability of zeolites constrains the upper reaction temperature to 800–850 °C.

Second, even in the confined micropores of HZSM-5 zeolite polyaromatic species are formed, eventually clogging the micropores and blocking the external surface.^[5] In fact, rapid catalyst deactivation is the main obstacle to overcome in commercializing this technology. Regeneration of the catalyst by burning off the coke is certainly possible, but a challenge here is that, in doing so at typical reaction temperatures, Mo-carbide species are reoxidized into mobile Mo-oxide species that react with aluminum framework atoms to form aluminum molybdate. This partially destroys the zeolite framework, resulting in irreversible deactivation.^[6] Thus, the few reported attempts made to regenerate Mo/HZSM-5 by oxygen have employed lower regeneration temperatures (500–550 °C) to retain the crystalline structure of the MoO₃/ZSM-5 catalyst.^[7] Temperature cycling in fixed-bed reactors is regarded as inefficient and, accordingly, it is no surprise that separating reaction and regeneration in different reactors has also been considered.^[8]

Herein, we demonstrate that supplying short pulses of oxygen to a continuous methane feed over a fixed bed containing Mo/HZSM-5 allows substantial stabilization of methane dehydroaromatization at a reaction temperature of 700 °C. By optimizing the O₂ pulsing frequency, chosen such that it is comparable to the assumed coke formation rate, the cumulative benzene yield was more than two times higher in comparison with a reference test with a methane-only feed.

The strategy is based on the presumption that oxygen can combust coke as long as it is still relatively young. Using

[*] Dr. N. Kosinov, F. J. A. G. Coumans, E. Uslamin, Prof. E. J. M. Hensen
Laboratory of Inorganic Materials Chemistry
Eindhoven University of Technology
P.O. Box 513, 5600 MB Eindhoven (The Netherlands)
E-mail: E.J.M.
E-mail: N.A.Kosinov@tue.nl
Hensen@tue.nl

Prof. F. Kapteijn
Catalysis Engineering, ChemE, Delft University of Technology
van der Maasweg 9, 2629 HZ Delft (The Netherlands)

Supporting information for this article can be found under:
<http://dx.doi.org/10.1002/anie.201609442>.

© 2016 The Authors. Published by Wiley-VCH Verlag GmbH & Co. KGaA. This is an open access article under the terms of the Creative Commons Attribution Non-Commercial License, which permits use, distribution and reproduction in any medium, provided the original work is properly cited, and is not used for commercial purposes.

^{13}C -labeled methane, we determined that oxygen molecules mainly react with surface carbon species and that oxidized molybdenum plays an important role in this process. At the applied conditions, the combustion of coke only produces synthesis gas (CO and H_2), which can be considered as a valuable side-product in the overall reaction scheme.

The Mo/HZSM-5 used was prepared by incipient wetness impregnation of HZSM-5 ($\text{Si}/\text{Al}=13$) with an aqueous solution of ammonium heptamolybdate, followed by calcination at 550°C . Performance of this catalyst was evaluated in a fixed-bed reactor at 700°C , with a methane weight hourly space velocity (WHSV) of 1.2 h^{-1} . O_2 pulses were delivered into this feed by an automated 6-way valve equipped with a 2 mL loop placed upstream of the reactor bed (Figure 1).

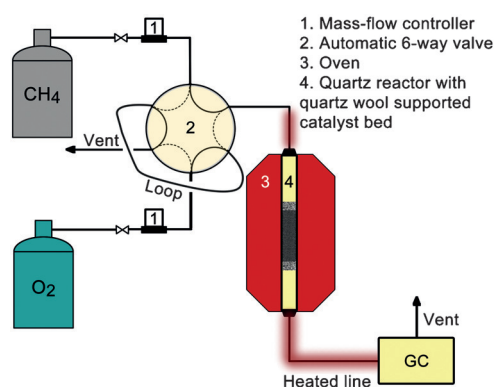


Figure 1. Experimental setup used for delivering O_2 pulses to CH_4 for pulsed in situ regeneration of Mo/HZSM-5 during methane dehydroaromatization.

Initially, we investigated the chemical reactions occurring during O_2 pulses in the CH_4 feed under dehydroaromatization conditions. For this purpose, the composition of the reactor effluent was analyzed by a mass spectrometer (MS). Figure 2a shows typical concentration profiles during a 2 mL O_2 pulse given during a catalytic reaction at 700°C . The dashed red profile corresponds to an O_2 pulse given to the same catalytic bed at room temperature, where no reaction takes place. It is characterized by an approximately 1 min long pulse (see high-resolution quantification by GC in the Supporting Information, Figure S1). At 700°C , the oxygen pulse is completely consumed and several products are observed over a period of several minutes. The main products are CO (m/z 28) and H_2 (m/z 2) with minor amounts of CO_2 (m/z 44) and H_2O (m/z 18). Production of CO is clearly associated with simultaneous consumption of O_2 . The CO diffuses through the bed nearly unperturbed compared to the room-temperature O_2 pulse because of its negligible interaction with the surface at 700°C .^[9] Molecular oxygen is involved in the oxidation of Mo_2C to MoO_3 and combustion of coke/hydrocarbon species, as described by the following Equations 1–5:

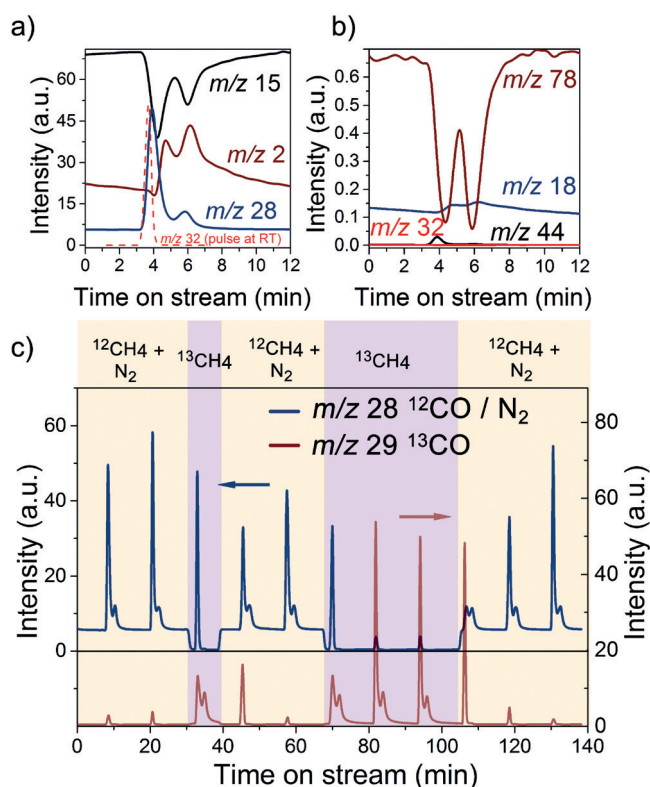


Figure 2. MS profiles of 2 mL O_2 pulses supplied to a 15 mL min^{-1} CH_4 flow over Mo/HZSM-5 at 700°C : a) major components are CO (m/z 28), H_2 (m/z 2), and CH_4 (m/z 15); the dashed line corresponds to a similar O_2 pulse supplied at ambient temperature (m/z 32); b) profiles of benzene (m/z 78), water (m/z 18), and CO_2 (m/z 44); no O_2 was detected at 700°C . c) ^{12}CO and ^{13}CO formation upon periodic oxygen pulsing and switching from $^{12}\text{CH}_4$ to $^{13}\text{CH}_4$ and vice versa.



The experiment does not allow distinguishing between CO and CO_2 as the primary product. If CO_2 is formed, then it can be converted by gasification of deposited coke into CO by reforming and Boudouard chemistry.^[10] Such secondary reactions of CO_2 explain the slight tailing of the peak compared to the O_2 pulse. The first H_2 peak stems from reforming of coke species by H_2O originating from coke combustion and it is delayed compared to the CO peak because of the stronger interaction of H_2O with the catalyst. Negative CH_4 and C_6H_6 peaks result from dilution of the methane feed when the O_2 pulse travels through the bed. These peaks are also slightly delayed compared to the first CO peak, which shows that CH_4 interacts with Mo-carbide through dissociative adsorption and recombinative desorption in its nearly equilibrated reaction to benzene and other products. After O_2 has been depleted molybdenum is recarbured (Equation 6), which explains the second CO and H_2 production and CH_4 consumption features after about 6 min.^[11]



Production of C_6H_6 also decreases during this period because CH_4 is consumed by the carburization process and considerable amounts of hydrogen evolved, thereby shifting the equilibrium. CH_4 , H_2 , and C_6H_6 features are delayed compared to that of CO because CH_4 interacts with the catalyst surface, whereas CO does not. The observation that C_6H_6 production proceeds after the O_2 pulse and before carburization occurs shows that not all Mo-carbide species have been oxidized. We had to limit the O/Mo ratio to 0.7 to avoid rapid deactivation of the catalyst.^[12] Ex situ XPS experiments show that the initial Mo^{VI} precursor in the fresh catalyst (Figure 3 a) is converted to Mo_2C in a methane flow (Figure 3 b). A sample taken out of the reactor during the regeneration reaction procedure with oxygen pulses contained a mixture of Mo^{VI} and Mo^{IV} oxides, as well as Mo_2C (Figure 3 c).

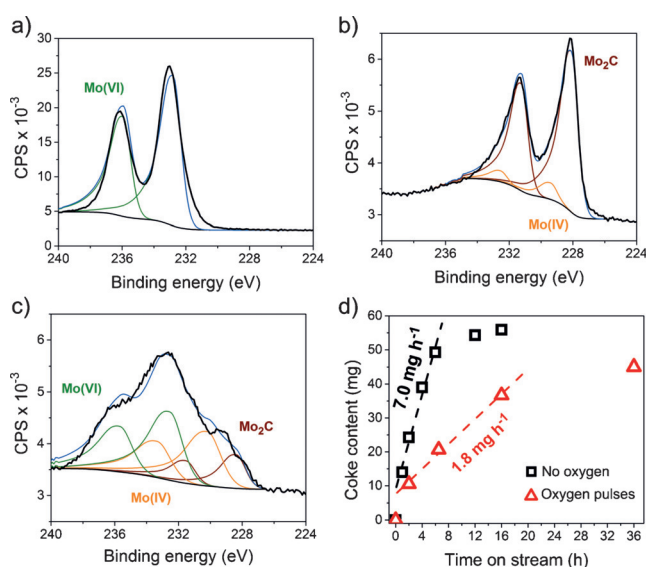


Figure 3. XPS spectra of a) as-prepared 5%Mo/HZSM-5, b) 5%Mo/HZSM-5 after 2 h in methane, and c) 5%Mo/HZSM-5 after 2 h in methane with O_2 pulses (2 mL every 12 min; sample quenched in He after eight pulses; corresponds to $t = 5$ min in Figure 2 a,b). d) Amount of coke formed on Mo/HZSM-5 under O_2 -free conditions and with 2 mL O_2 pulses every 12 min.

Isotopic labeling of methane was employed to distinguish the relative contributions of the solid and gas phases to conversion of O_2 . For this purpose, we pulsed 2 mL of O_2 to the catalyst bed every 12 min, alternating with a flow mixture of $^{12}\text{CH}_4:\text{N}_2$ (95:5; N_2 was used as an internal standard) and pure $^{13}\text{CH}_4$ (Figure 2 c), while monitoring m/z 28 (^{12}CO and N_2) and m/z 29 (^{13}CO) MS signals. The experiment was first carburized in $^{12}\text{CH}_4/\text{N}_2$ at 700°C for 0.5 h. The first two O_2 pulses each lead to two consecutive ^{12}CO peaks similar to the experiment described in Figure 2 a. The size of the ^{13}CO peak observed in this experiment is consistent with the natural abundance of ^{13}C . After switching the feed to $^{13}\text{CH}_4$ and complete removal of $^{12}\text{CH}_4$ from the reactor (as evidenced by absence of the m/z 28 N_2 signal), another O_2 pulse was given.

In this case, the first CO combustion peak appears mainly in the form of ^{12}CO together with a relatively small ^{13}CO signal. This implies that O_2 was mainly used to oxidize ^{12}C present on the catalyst, while the contribution of oxidation of the gas-phase $^{13}\text{CH}_4$ feed, or ^{13}C -containing reaction intermediates and products, was minor. On the other hand, the second CO peak was pure ^{13}CO , which shows that $^{13}\text{CH}_4$ was used to carburize MoO_3 back to the carbide form. Switching to $^{12}\text{CH}_4$ and providing another O_2 pulse to the bed led to similar events, with ^{13}CO dominating the combustion and ^{12}CO the carburization. MS data quantification allowed estimation of the relative contributions of Mo_2C oxidation (ca. 21%), coke oxidation (ca. 62%), and oxidation of gas-phase hydrocarbons (ca. 18%) to the consumption of O_2 (Supporting Information, Figure S5). Thus, O_2 was mainly used to oxidize Mo-carbide and coke, while combustion of gaseous methane and reaction products, such as ethylene and benzene, was only minor.

To prove the effectiveness of O_2 pulsing in coke removal, we used thermogravimetric analysis (TGA) to determine the coke content with increasing time-on-stream; for a conventional reaction experiment and one in which 2 mL oxygen were delivered every 12 min. Figure 3 d shows that the rate of coke formation is substantially lower in the pulsed case. Leveling off of coke content after prolonged reaction is due to catalyst deactivation. The oxygen balance shows that the atomic ratio of $\text{C}_{\text{coke-combusted}}/\text{O}_{\text{pulsed}}$ is approximately 0.55, in good agreement with the value obtained by isotopic labeling (0.62).

To optimize the amount of O_2 delivered to the catalyst bed, we varied the pulsing frequency from $1/12 \text{ min}^{-1}$ to $1/2 \text{ min}^{-1}$ (denoted: 2/12, 2 mL every 12 min; 2/6, 2 mL every 6 min; and so forth). The results are collected in Figure 4 and highlight increased catalyst stability compared to the O_2 -free reference experiment for the 2/12, 2/6, and 2/3 experiments. In the 2/12 experiment, the cumulative benzene yield (integrated over 16 h on stream) is about 50% higher than in the reference experiment. When the frequency is increased to 2/6 and 2/3, the catalytic performance at early reaction times is lower because of the frequent oxidation of the Mo-carbide phase, but this comes with greatly improved stability during prolonged operation. Overall, the cumulative benzene yield is two times higher than that of the reference. For the 2/2 experiment, the benzene yield is decreased and CO became the main product because CH_4 was mainly used to recarburize the oxidized catalyst. At the optimum (between 2/6 and 2/3), the O_2 amount fed to the catalyst is high enough to remove a substantial amount of coke, yet low enough to avoid over-oxidation and destabilization of the catalyst.

Experiments involving continuous addition of 2 vol% O_2 to the feed or intermittent calcination at 700°C led to rapid deactivation (Supporting Information, Figure S8), showing the promise of O_2 pulsing for in situ catalyst regeneration. The CO and H_2 side-products come in a proportion close to 1:2 (Figure 4 f) and can be used to produce chemicals or transportation fuels.^[13] In the 2/3 experiment, the catalyst retained some activity even after 65 h on stream (Supporting Information, Figures S11–S13). Nevertheless, deactivation by coking cannot be completely suppressed, which is likely a

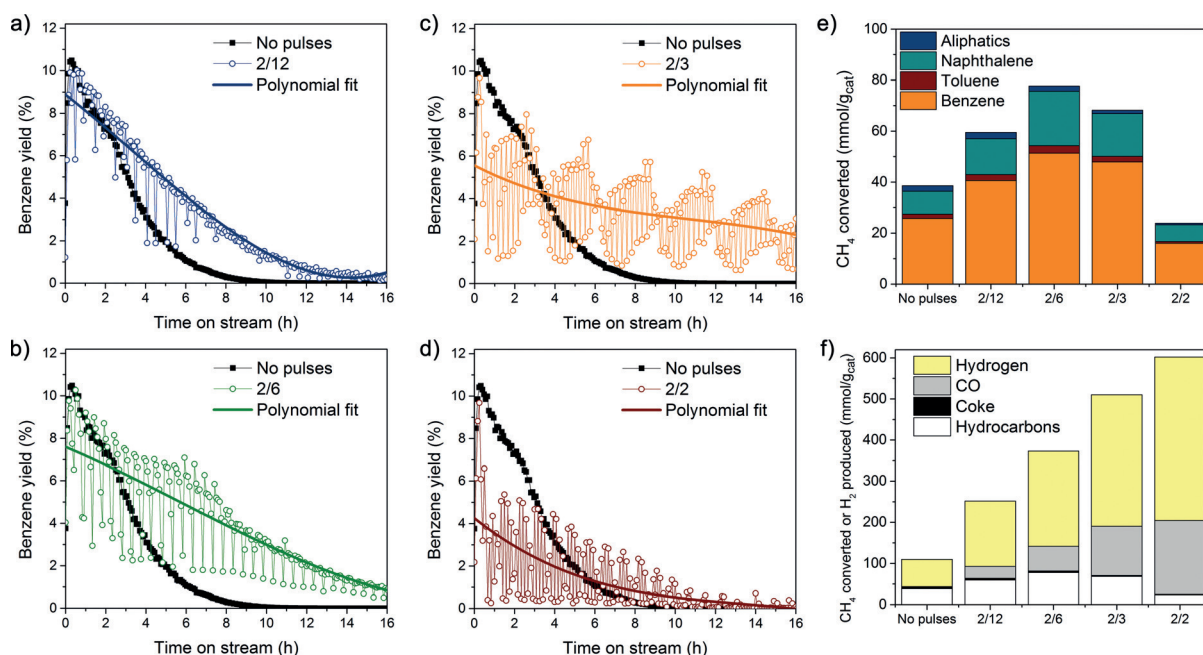


Figure 4. Benzene yield as a function of time on stream at O₂-pulsing frequencies of a) 2 mL/12 min, b) 2 mL/6 min, c) 2 mL/3 min, and d) 2 mL/2 min. The variation in benzene yield relates to the difference in GC analysis time (5 min) and the O₂-pulsing frequency. Full colored lines represent averaged benzene yield (for a detailed explanation see the Supporting Information, Figures S1–S4). Product distribution at different frequencies: e) hydrocarbon products; f) hydrocarbons, coke, CO, and hydrogen. Reaction conditions: 0.5 g Mo/HZSM-5, 700 °C, CH₄ WHSV = 1.2 h⁻¹, t = 16 h, O₂ pulsing started after the catalyst was carburized for 0.5 h at 700 °C.

consequence of the ageing of the coke and the integral reactor operation resulting in non-uniform regeneration. Indeed, it is known that with increasing time-on-stream more recalcitrant “hard” coke is formed.^[14]

By TGA, we established that Mo₂C is the most reactive component towards oxidation in the working Mo/HZSM-5 catalyst (Supporting Information, Figure S6). These data show that MoO₃ catalyzes the oxidation of coke (Supporting Information, Figure S7), implying that “soft” coke located in close proximity to molybdenum species can be removed more easily than “hard” coke, which is formed in the vicinity of Brønsted acid sites.^[15] The catalytic activity of Mo/HZSM-5 was fully restored after 16 h on stream in the 2/6 experiment by air calcination at 550 °C for 2 h (Figure 5). Elemental analysis confirmed that no molybdenum was lost as volatile MoO₃ during the O₂ pulsing, while XRD confirms that the intermittent regeneration of MoO₃ did not degrade the zeolite framework as it does during calcination in air at 700 °C (Supporting Information, Figures S9 and S10).

In summary, this work presents a novel method to improve the efficiency of methane dehydroaromatization at relevant reaction conditions. Periodic supply of short pulses of oxygen into the methane feed at optimized frequency leads to doubling of the benzene yield, while the only non-hydrocarbon side-product is syngas with a H₂/CO ratio of close to two. Selective reaction of oxygen with the surface species (coke, carbide, and so on) lies at the origin of this online in situ regeneration approach. Less than one-fifth of supplied oxygen reacts with the gas-phase reactant and products. As a result, the rate of coke formation is decreased four times as compared to oxygen-free conditions. Oxidation of

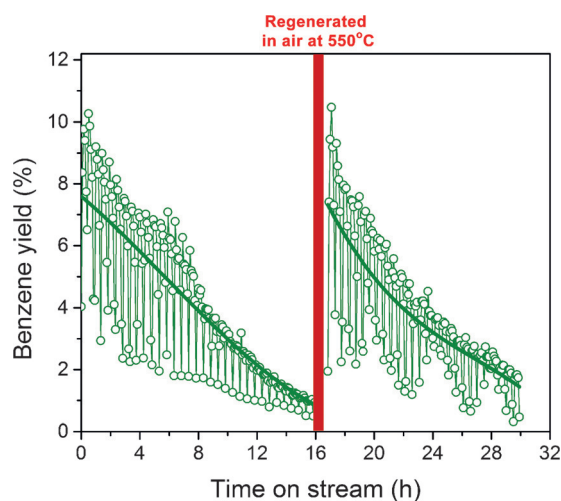


Figure 5. Benzene yield as a function of time on stream for a 5% Mo/HZSM-5 catalyst during 2 mL/6 min O₂ pulsing. After 16 h on stream the catalyst was cooled to 550 °C, regenerated in a flow of air for 2 h, and then tested again with 2 mL/6 min O₂ pulsing. Reaction conditions: 0.5 g Mo/HZSM-5, 700 °C, CH₄ WHSV 1.2 h⁻¹, periodic 2 mL/6 min O₂ pulsing.

Mo-carbide to Mo-oxide is key to the selective combustion of coke species. Rapid cycling between the oxidic and carbidic forms of molybdenum does not affect the catalyst in a negative manner (no framework damage, no loss of molybdenum) and this is likely due to the stabilization of molybdenum-oxo complexes on cation-exchange sites of the zeolite.^[7b] Thus, it is possible to combine the online pulsing operation of methane

dehydroaromatization with periodic regeneration by air calcination at 550 °C.^[7a] The next step is to explore suitable reactor configurations to realize this novel concept.

Acknowledgements

Financial support from the SABIC-NWO CATC1CHEM/CHIPP project is gratefully acknowledged. We thank Dr. Christoph Dittrich (SABIC), Dr. Frank Mostert (SABIC), Dr. Xander Nijhuis (SABIC), Prof. Dr. Jorge Gascon (TU Delft) and Ina Vollmer (TU Delft) for fruitful discussion.

Keywords: arenes · catalyst deactivation · catalyst regeneration · methane dehydroaromatization · Mo/HZSM-5

How to cite: *Angew. Chem. Int. Ed.* **2016**, *55*, 15086–15090
Angew. Chem. **2016**, *128*, 15310–15314

- [1] a) A. I. Olivos-Suarez, Á. Szécsényi, E. J. M. Hensen, J. Ruiz-Martínez, E. A. Pidko, J. Gascon, *ACS Catal.* **2016**, *6*, 2965–2981; b) P. Tang, Q. Zhu, Z. Wu, D. Ma, *Energy Environ. Sci.* **2014**, *7*, 2580–2591; c) S. Majhi, P. Mohanty, H. Wang, K. K. Pant, *J. Energy Chem.* **2013**, *22*, 543–554; d) X. Guo, G. Fang, G. Li, H. Ma, H. Fan, L. Yu, C. Ma, X. Wu, D. Deng, M. Wei, D. Tan, R. Si, J. Li, L. Sun, Z. Tang, X. Pan, X. Bao, *Science* **2014**, *344*, 616–619; e) F. Jiao, J. Li, X. Pan, H. Li, M. Wei, Y. Pan, Z. Zhou, M. Li, S. Miao, J. Li, Y. Zhu, D. Xiao, T. He, J. Yang, F. Qi, Q. Fu, X. Bao, *Science* **2016**, *351*, 1065–1069.
- [2] a) Z. R. Ismagilov, E. V. Matus, L. T. Tsikoza, *Energy Environ. Sci.* **2008**, *1*, 526–541; b) J. J. Spivey, G. Hutchings, *Chem. Soc. Rev.* **2014**, *43*, 792–803; c) L. Li, X. Mu, W. Liu, X. Kong, X. Kong, S. Fan, Z. Mi, C.-J. Li, *Angew. Chem. Int. Ed.* **2014**, *53*, 14106–14109; *Angew. Chem.* **2014**, *126*, 14330–14333; d) D. Ma, Y. Shu, M. Cheng, Y. Xu, X. Bao, *J. Catal.* **2000**, *194*, 105–114; e) D. Ma, Y. Lu, L. Su, Z. Xu, Z. Tian, Y. Xu, L. Lin, X. Bao, *J. Phys. Chem. B* **2002**, *106*, 8524–8530.
- [3] O. V. Bragin, T. V. Vasina, A. V. Preobrazhenskii, K. M. Mina-chev, *Bull. Acad. Sci. USSR Div. Chem. Sci.* **1989**, *38*, 680.
- [4] M. Guisnet, P. Magnoux, *Appl. Catal. A* **2001**, *212*, 83–96.
- [5] a) Y. Song, Y. Xu, Y. Suzuki, H. Nakagome, X. Ma, Z. G. Zhang, *J. Catal.* **2015**, *330*, 261–272; b) Y. Xu, Y. Song, Y. Suzuki, Z.-G. Zhang, *Catal. Sci. Technol.* **2013**, *3*, 2769–2777; c) B. M. Weckhuysen, M. P. Rosynek, J. H. Lunsford, *Catal. Lett.* **1998**, *52*, 31–36; d) D. Ma, D. Wang, L. Su, Y. Shu, Y. Xu, X. Bao, *J. Catal.* **2002**, *208*, 260–269.
- [6] a) I. Lezcano-González, R. Oord, M. Rovezzi, P. Glatzel, S. W. Botchway, B. M. Weckhuysen, A. M. Beale, *Angew. Chem. Int. Ed.* **2016**, *55*, 5215–5219; *Angew. Chem.* **2016**, *128*, 5301–5305; b) Z. Cao, H. Jiang, H. Luo, S. Baumann, W. A. Meulenber, J. Assmann, L. Mleczko, Y. Liu, J. Caro, *Angew. Chem. Int. Ed.* **2013**, *52*, 13794–13797; *Angew. Chem.* **2013**, *125*, 14039–14042; c) D. Ma, Y. Shu, X. Han, X. Liu, Y. Xu, X. Bao, *J. Phys. Chem. B* **2001**, *105*, 1786–1793; d) V. T. T. Ha, A. Sarioglan, A. Erdem-Senatalar, Y. Ben Taarit, *J. Mol. Catal. A* **2013**, *378*, 279–284; e) S. H. Morejudo, R. Zanon, S. Escolastico, I. Yuste-Tirados, H. Malerod-Fjeld, P. K. Vestre, W. G. Coors, A. Martínez, T. Norby, J. M. Serra, C. Kjolseth, *Science* **2016**, *353*, 563–566.
- [7] a) M. T. Portilla, F. J. Llopis, C. Martínez, *Catal. Sci. Technol.* **2015**, *5*, 3806–3821; b) J. Gao, Y. Zheng, J. Jehng, Y. Tang, I. E. Wachs, S. G. Podkolzin, *Science* **2015**, *348*, 686–690; c) C. H. L. Tempelman, M. T. Portilla, M. E. Martínez-Armero, B. Mezari, N. G. R. de Caluwe, C. Martínez, E. J. M. Hensen, *Microporous Mesoporous Mater.* **2016**, *220*, 28–38.
- [8] a) C. Dittrich, A process for carrying out endothermic, heterogeneously catalyzed reactions, WO2015082375 A1, June 11, **2015**; b) L. L. Iaccino, T. Xu, J. S. Buchanan, N. Sangar, J. J. Patt, M. A. Nierode, K. R. Clem, M. Afeworki, Production of aromatics from methane, US7589246 B2, September 15, **2009**; c) L. L. Iaccino, N. Sangar, E. L. Stavens, M. J. Vincent, Process for methane conversion, US7781636 B2, August 24, **2010**.
- [9] Z. Liu, M. A. Nutt, E. Iglesia, *Catal. Lett.* **2002**, *81*, 271–279.
- [10] a) J. Bai, S. Liu, S. Xie, L. Xu, L. Lin, *Catal. Lett.* **2003**, *90*, 123–130; b) L. Wang, R. Ohnishi, M. Ichikawa, *J. Catal.* **2000**, *190*, 276–283; c) S. Liu, Q. Dong, R. Ohnishi, M. Ichikawa, *Chem. Commun.* **1998**, 1217–1218.
- [11] a) H. S. Lacheen, E. Iglesia, *Phys. Chem. Chem. Phys.* **2005**, *7*, 538–547; b) D. Ma, Y. Shu, W. Zhang, X. Han, Y. Xu, X. Bao, *Angew. Chem. Int. Ed.* **2000**, *39*, 2928–2931; *Angew. Chem.* **2000**, *112*, 3050–3053.
- [12] P. L. Tan, Y. L. Leung, S. Y. Lai, C. T. Au, *Catal. Lett.* **2002**, *78*, 251–258.
- [13] a) E. Jin, Y. Zhang, L. He, H. G. Harris, B. Teng, M. Fan, *Appl. Catal. A* **2014**, *476*, 158–174; b) J. Sun, G. Yang, Y. Yoneyama, N. Tsubaki, *ACS Catal.* **2014**, *4*, 3346–3356; c) H. M. T. Galvis, K. P. de Jong, *ACS Catal.* **2013**, *3*, 2130–2149.
- [14] C. H. L. Tempelman, E. J. M. Hensen, *Appl. Catal. B* **2015**, *176–177*, 731–739.
- [15] a) S. S. Masiero, N. R. Marcilio, O. W. Perez-Lopez, *Catal. Lett.* **2009**, *131*, 194–202; b) C. H. L. Tempelman, V. O. De Rodrigues, E. R. H. Van Eck, P. C. M. M. Magusin, E. J. M. Hensen, *Microporous Mesoporous Mater.* **2015**, *203*, 259–273.

Received: September 26, 2016

Revised: October 16, 2016

Published online: October 28, 2016